Chemical Engineering Journal 281 (2015) 782–792

Contents lists available at ScienceDirect

Chemical Engineering Journal

journal homepage: www.elsevier.com/locate/cej

Immobilized Nanopillars-TiO_2 in the efficient removal of micro-pollutants from aqueous solutions: Physico-chemical studies

C. Lalhriatpuia [a], Diwakar Tiwari [a,*], Alka Tiwari [b], Seung Mok Lee [b]

[a] Department of Chemistry, School of Physical Sciences, Mizoram University, Aizawl 796004, India
[b] Department of Health and Environment, Catholic Kwandong University, 522 Naegok-dong, Gangneung, Gangwon-do 210-701, Republic of Korea

HIGHLIGHTS

- Nano-pillars TiO_2 immobilize onto borosilicate glass using sol–gel template method.
- Thin films with and without filler (PEG) is well characterized.
- Thin films are utilized in the photocatalytic degradation of micro-pollutants.
- Physico-chemical studies enabled to deduce mechanism of degradation.

GRAPHICAL ABSTRACT

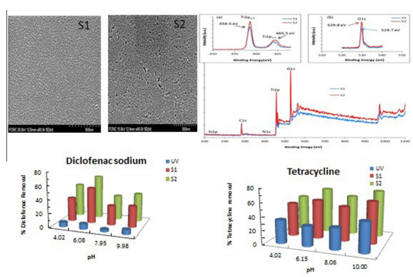

Thin Films of nano-TiO_2 was obtained with and without PEG (S2 and S1) and utilized in the photocatalytic degradation of micro-pollutants

ARTICLE INFO

Article history:
Received 30 May 2015
Received in revised form 8 July 2015
Accepted 9 July 2015
Available online 13 July 2015

Keywords:
Immobilized Nano-pillars-TiO_2
Tetracycline
Diclofenac
Photocatalyst
Mineralization
Kinetics

ABSTRACT

Nanopillars-TiO_2 was immobilized onto a borosilicate glass disk using sol–gel template method. The TiO_2 film was immobilized with and without polyethylene glycol as filler media and annealed at 500 °C. The prepared films were characterized by the IR, XRD, XRF and XPS analytical methods. The surface morphology was obtained using FE-SEM and AFM images of these thin films and the BET specific surface area was obtained. Further, the Nanopillars TiO_2 was employed in the photocatalytic degradation of micro-pollutants *viz.*, diclofenac sodium and tetracycline hydrochloride from aqueous solutions using UV-light under batch reactor operations. Various physico-chemical parametric studies *viz.*, effect of pH, pollutant concentration and interfering ions was studied to deduce the mechanism involved in photocatalytic degradation of these pollutants. The time dependence degradation of these pollutants provided kinetics of degradation of these pollutants from aqueous solutions. The studies were further extended with total organic carbon measurement using TOC analyser to demonstrate an apparent mineralization of these pollutants. The photocatalytic degradation was assessed in presence of scavengers and several co-existing ions to simulate the data for real wastewater matrix. The hydroxyl radical scavengers 2-propanol and sodium bicarbonate greatly suppressed the catalytic activity of the thin films. However, the singlet oxygen scavenger sodium azide could not affect significantly the catalytic activity of these thin films at least the degradation of diclofenac sodium and tetracycline from aqueous solutions.

1. Introduction

Presence of organic micro-pollutants, in particular variety of pharmaceuticals and personal care products (PPCPs), seemingly

* Corresponding author. Tel.: +91 9862323015; fax: +91 389 2330834.
E-mail address: diw_tiwari@yahoo.com (D. Tiwari).

http://dx.doi.org/10.1016/j.cej.2015.07.032
1385-8947/

pose serious environmental concerns during recent past; since several micro-pollutants are persistent, low biodegradable and toxic even at low level. A widespread occurrence of PPCPs is demonstrated by a number of monitoring agencies and measurable concentration of many of the PPCPs are detected in the wastewater, surface water, sediments, groundwater, and even in drinking water [1]. PPCPs enter into the terrestrial environment through direct runoff and excretion of un-metabolized drugs or active metabolites and/or degradation by-products [2]. It was reported that *Ca* 70% of consumed pharmaceuticals were excreted through human urine as active ingredients or metabolites [3,4]. The normal sewage treatment system is insufficient to eliminate such pollutants completely, which results in presence of residual load of pollutants in the effluent water [5].

Tetracycline (TC; Structure 1) is an antibiotic drug widely prescribed for the treatment of bacterial infections [6]. TC is employed in aquaculture and livestock industry as one of typical antibiotic [7], food additives and growth promoters in farming and animal husbandry [8]. The consumption of tetracycline for veterinary purposes is higher than for other classes of antibiotics [9]. Similarly, diclofenac (2-[-2′,6′-(dichlorophenyl)amino]phenyl acetic acid) (Structure 2), used mostly to its sodium salt, is a non-steroidal anti-inflammatory drug (NSAID) widely employed for the treatment of inflammatory and painful diseases of rheumatic, nonrheumatic and antiarthritic origin. It is recommended to reduce menstrual pain, dysmenorrhea etc. An annual consumption of diclofenac is *Ca* 940 tons globally with a recommended dose of 100 mg/day [10,11]. The continued intake of diclofenac, at low level, by humans shows several adverse biochemical effects e.g., cytotoxicity to liver, kidney and gill cells as well the renal lesions even at a concentration of 1.0 μg/L [12–15]. It may also influence the biochemical functions of fish which leads to tissue damage [16].

Therefore, there is greater attention of effective and efficient remediation of aquatic environment contaminated with micro-pollutants. The low solubility, high log K_{ow} values, low dipole moments and negative charges makes high rejection values for diclofenac in the nano-filtration unit [17]. The unit operations associated with ozonation [18], adsorption on activated carbon [19,20] and membrane filtration as nano-filtration and reverse osmosis [21,22] are some of possible ways as employed in the removal of several pharmaceuticals (>99%). The degradation of diclofenac from aqueous solutions as a combination of membrane TiO_2/UV-A catalysis-ultrafiltration with photolysis could allow an effective and efficient diclofenac degradation [23]. The oxygen and free radical promoters are investigated in the photolysis (UV-254) of diclofenac [24]. Chlorine dioxide (ClO_2) is employed in degradation of diclofenac under the simulated water disinfection condition. Results reveal that rapid and significant degradation of diclofenac occurs during initial few minutes but much longer time is needed for its complete mineralization [25]. Similarly, photocatalytic ozonation (O_3/UVA/TiO_2) is assessed in the degradation of diclofenac and shows that a complete elimination of diclofenac is achieved within 6 min and from 60% to 75% of TOC is removed within 60 min of operation [26]. An advanced oxidation/reduction process is conducted using a pulse radiolysis having 8 MeV accelerator which produces 2 ns electron pulse causes a production of high concentration of radicals i.e., 1 mM per pulse. The kinetics, degradation pathways along with the toxicity is obtained for diclofenac with this study [27]. The presence of different forms of nitrogen is studied in the photo degradation of diclofenac under the simulated sunlight. Results show that the degradation of diclofenac proceeds with pseudo-first order rate kinetics [28]. *In vivo* and *in vitro* studies conducted on the white-rot fungus *Trametes versicolor* pellets show almost a complete oxidative removal of diclofenac is obtained within short period of time [29].

On the other hand, tetracycline is having a 4-ring system. It contains multiple ionisable functional groups. TC possesses three pK_a values due to the tricarbonylamide, phenolic diketone and dimethylamino groups, respectively. Literature reveals that various methods were demonstrated in the degradation of tetracycline from aqueous solutions. A boron doped diamond electrode was used in a complete degradation of TC using electrochemical reactor operated at constant current density of 300 A/m^2 [30]. Similarly, Electrochemical Oxidation (EO) and Electro-Fenton (EF) processes were assessed in the oxidation of TC. It was reported that the EO process contained with carbon-felt cathode was relatively more efficient than the stainless steel cathode. Further, almost a total mineralization (TOC removal up to 98%) of 100 mg/L of TC was obtained with 6 h operation using either EO and/or EF treatment using a BDD anode [31]. A photo-electro-Fenton process was proposed using a fabricated Fe_3O_4–graphite cathode and a high degradation of TC was achieved and interestingly the electrode could be reused with a similar efficiency [32]. Fe(III) via complexation with the TCs promotes the degradation of several TCs even in absence of light sources [33]. Similarly, the combined application of nano-TiO_2 and corona discharge plasma was utilized in the catalytic degradation of TC (50 mg/L) from aqueous solutions and the TC removal was achieved to 85.1% using the input discharge power of 36.0 W [34]. The nano-TiO_2(P25) was introduced in the photocatalytic reactor for the oxidation of TC and one of the end products NH_4^+ was detected [35]. Photooxidation of TC was enhanced in presence of H_2O_2. Moreover, the presence of dissolved organic matter greatly enhanced the degradation of TC possibly due to the formation of radical species $^{\cdot}OH$ which acted as strong photosensitizer [36]. The visible light driven photocatalysts *viz.*, Ag-decorated $K_2Ta_2O_6$ nanocomposite, $Ni_{(1-x)}Cu_{(x)}Fe_2O_4$ or Sr–Bi_2O_3 were assessed in the photocatalytic degradation of TC from aqueous solutions and found to be efficient in the treatment process [2,37,38]. Although, the use of nano-TiO_2 in the photocatalytic degradation of several micro-pollutants is found to be efficient however; separation of catalyst from the bulk phase or repeated use of catalyst restricts its wider implication in the wastewater treatment plants.

Therefore, the present investigation deals to immobilize the Nanopillars-TiO_2 onto a borosilicate glass substrate using the template sol–gel synthetic process. Further, the materials were utilized in the photocatalytic degradation of micro-pollutants *viz.*, diclofenac sodium and tetracycline hydrochloride from aqueous solutions.

2. Materials and methods

2.1. Chemical and materials

Titanium (IV) isopropoxide, poly(ethylene glycol), diclofenac sodium salt and tetracycline hydrochloride were procured from the Sigma Aldrich. Co., USA. Acetylacetone (assay ⩾ 99%), ethanol anhydrous, hydrochloric acid, sodium hydroxide, zinc chloride, cupric sulfate pentahydrate, cadmium nitrate tetrahydrate, ethylenediaminetetraacetic acid, sodium nitrate, sodium nitrite, oxalic acid, glacial acetic acid, HPLC water, sodium azide, sodium bicarbonate, 2-propanol and acetonitrile (HPLC grade) were obtained from the Merck India Ltd., India. Sodium chloride and glycine were procured from the Himedia, India Ltd., India. Purified water (18.2 MΩ · cm at 25 °C) was obtained from the Millipore Water Purification system (Model: Elix 3) and used for entire solution preparations and other analytical studies.

A pH-meter having glass and calomel electrode assembly (Thermo Scientific, Sn B43460) was used for pH measurements. UV–Vis spectrophotometer (Thermo Electron Corporation, England; Model: Thermo Spectronic UV1) was employed to study the degradation kinetics of organic compounds as measuring the change in concentration at a fixed wavelength (276 nm for DFS and 360 nm for tetracycline). Calibration line for these pollutants i.e., TC and DFS was obtained using their standard solutions having the concentrations of 0.1, 1.0, 5.0, 10.0 and 15.0 mg/L. Reasonably a good linearity was obtained between the pollutant concentration and absorbance as $R^2 = 0.999$. The TOC Analyzer (Shimadzu, Japan; Model : TOC-VCPH/CPN) was fully employed to obtain the total organic carbon content data to study the degradation of organic compounds present in water. Similarly, the HPLC Instrument (Model: Waters 515 HPLC pump, Detector: Waters 2489 UV/Visible Detector, Column: Symmetry® C18 5 μm (4.6 × 250 mm column)) was employed for the quantitative determination of diclofenac sodium. The acetonitrile (70%) + water (29%) + glacial acetic acid (1%) by v/v were used as mobile phase and the absorbance intensity was measured at 276 nm. Standard calibration of DFS by the HPLC measurements were found to be extremely good since the straight line was having R^2 values >0.999.

2.2. Methodology

2.2.1. Preparation of titania sol solutions

Two types of Nanopillars-TiO_2 were prepared using simple sol–gel process and named as T1 and T2. T1 was prepared dissolving titanium isopropoxide (TISP) in acetyl-acetone (AcAc) in order to control the hydrolysis and condensation reactions. Then, ethanol (EtOH), acetic acid (AcOH) and distilled water (H_2O) were added drop-wise to this solution to start hydrolysis and condensation reactions. The solution was stirred vigorously for 2 h and was sonicated for 30 min. The obtained sol was aged for 1 day prior to use it for thin film preparation or immobilization. The amount of these chemicals: TISP: AcAc: EtOH: AcOH: H_2O was taken as: 2.8 g: 1.3 g: 18.4 g: 0.58 g: 2.25 g, respectively.

A similar process was used to prepare titania T2 but added with 2 g of poly(ethylene glycol) (PEG) (average molecular weight 8000) maintaining the previous molar ratios of precursors as constant.

2.2.2. Preparation of Nanopillars-TiO_2 thin films

Two very cleaned and dried borosilicate circular glass disks (2.3 cm diameter and 0.5 mm thickness) were dipped into transparent orange color T1 and T2 sol solutions, separately and were kept in it (in vertical position) for 1 h. It was removed slowly and placed it in air at room temperature for 12 h. Thin film of TiO_2 was formed onto the substrate surfaces and it was then dried first at 100 °C for 1 h and subsequently was annealed at 500 °C for 3 h in an electric furnace (Nabertherm; Model No. LT/15/12/P330, Germany). The dipping process was repeated three times for both solutions in order to obtain homogeneous thin films onto the substrate surface. The Nanopillars-TiO_2 thin films were obtained, S1 (TiO_2 film without PEG) and S2 (TiO_2 film with PEG), which were kept in a closed and dry container under dark condition for further use.

2.2.3. Characterization of thin films

Surface morphology of S1 and S2 samples was obtained using SEM (Scanning Electron Microscope) machine (Model FE-SEM SU-70, Hitachi, Japan). X-ray diffraction (XRD) data was collected by the X-ray diffraction machine (i.e., PANalytical, Netherland; Model X'Pert PRO MPD). The diffraction data was recorded at a scan rate of 0.034 of 2θ illumination and at an applied voltage of 45 kV with a measured current 35 mA. The Cu K_α radiation was employed having a wavelength of 1.5418 Å. The elemental composition of thin films along with borosilicate glass substrate was obtained employing the X-ray Fluorescence (XRF) spectrometer (Model: ZSX 100e, Rigaku, Japan). AFM measurements were carried out in a non-contact mode, using the XE-100 apparatus from Park Systems (2011) having sharp tips (>8 nm tip radius; PPP-NCHR type from Nanosensors™). The topographical 3D AFM images were taken over the area of 10 × 10 μm^2. XPS (X-ray Photoelectron Spectroscopy) analysis was conducted using a Theta probe AR-XPS system (Thermo Fisher Scientific East Grinstead, UK), using an AlK_α monochromatic radiation ($h\nu = 1486.6$ eV) at a power of 150 W with a spot size of 400 μm. The aliphatic C peak at 284.6 eV was used as a binding energy reference. FT-IR (Bruker, Tensor 27, USA by KBR disk method) was used to collect the IR data for these thin films. Moreover, the BET specific area was obtained using Protech Korea BET surface area Analyzer (Model ASAP 2020).

2.2.4. pH_{PZC} measurements

The pH_{PZC} (point of zero charge) of the two powder samples P1 and P2 was determined using the pH drift method reported previously [39].

2.2.5. Photo-catalytic degradation experiment

Photo-catalytic degradation of diclofenac sodium (DFS) or tetracycline (TC) was carried out under the batch reactor experimentation. The reactor was composed with a black box (dimension: 60 × 45 × 45 cm). A 150 mL borosilicate glass beaker containing 50.0 mL of pollutant solution having the known concentration of DFS/or TC was taken and thin film (S1) or (S2) (2.3 cm diameter and 0.5 mm thickness) was placed horizontally at the bottom and center of the reactor. An UV-C lamp, maximum wavelength (λ) = 253.7 nm (Model: Phillips TUV 11W, 4 P.SE; Poland), was placed at the top of the reactor at 10 cm above the solution. The UV-radiation enters the TiO_2 photocatalyst through the pollutant solution, causing the photocatalytic oxidation process. The reaction temperature was maintained at 25 ± 1 °C using a self-assembled water-bath. Air was bubbled to the reactor solution using aquarium air pump. The samples were taken from the reactor at certain time intervals and the pollutant concentration was analyzed with a UV–Vis spectrophotometer or otherwise the final pollutant concentration after 2 h irradiation was determined employing HPLC (for DFS). Initially, blank experiments were performed under UV irradiation without TiO_2 photocatalyst for comparison. Moreover, parallel experiments were performed in dark using the S1 or S2 disks dipped in the pollutant solutions i.e., DFS or TC (1.0 mg/L) for 2 h and then the solutions were subjected for the HPLC or UV–Vis measurements. No significant change in pollutant concentration was obtained.

Stock solutions of DFS (20.0 mg/L) or TC (50.0 mg/L) was prepared in purified water. The solution was sonicated for 10 min to increase the solubility of these pollutants in water. Further, the required experimental concentration was obtained by the successive dilution of stock solutions. The pH of these solutions was maintained with dropwise addition of conc. HCl/NaOH solutions. The concentration dependence data was obtained varying the DFS or TC concentrations respectively from 1.0 to 5.0 mg/L and 1.0 to 20.0 mg/L. The percent efficiency of degradation of DFS or TC was calculated using Eq. (1):

$$Percent\ Removal = \frac{C_i - C_f}{C_i} \times 100 \quad (1)$$

where C_i and C_f are the concentrations of DFS/or TC before and after the photocatalytic treatment.

3. Results and discussion

3.1. Characterization of thin films

XRD results were obtained for the S1 and S2 samples and returned in Fig. 1S or elsewhere [40]. The samples S1 and S2 showed characteristics peaks at the 2θ values of 25.39, 37.84, 48.14, 53.44 and 54.59 which is well matched with the anatase phase of TiO_2. No characteristic peak of rutile phase was observed. It was mentioned that among the crystalline phases of TiO_2, anatase is most active photocatalyst [41].

The average particle size (D) of the TiO_2 was calculated using the Debye–Scherrer equation (2):

$$D = \frac{0.89 \cdot \lambda}{B \cdot \cos \theta} \tag{2}$$

where λ is the incident wavelength of the X-rays, B and θ are the full width at half maxima and semi-angle of diffraction corresponding to the most intensive diffraction peak, respectively. The size of particles are calculated for S1 and S2 catalysts and found to be 25.4 and 21.9 nm, respectively. This further indicates that the S1 and S2 comprised with Nanosized, possibly the Nanopillars TiO_2, which evenly distributed on to the substrate surface.

FT-IR results for S1 and S2 are presented graphically in Fig. 2S or elsewhere [40]. Both the IR spectra obtained for the S1 or S2 are almost identical in nature; showing sharp band at around 3437 cm^{-1} assigned to the O—H stretching vibration of Ti—OH [42]. The bending vibration of O—H mode is obtained at the wavenumber of around 1638 cm^{-1}. The bands at the region of 470 and 422 cm^{-1} are assigned to bending vibrations of Ti—O and Ti—O—Ti of the titanium dioxide framework [43] or perhaps the stretching mode of Ti—O bond which is enveloped with the bonds of Ti—O—Ti [44]. While narrow bands at 2922 and 2862 cm^{-1} are attributed to the organic residues present with the TiO_2 template preparation [45].

Similarly, the SEM images of S1 and S2 were included in Fig. 3S also presented elsewhere [40]. The image of S1 catalyst shows that Nanosized pillars of TiO_2 are aggregated onto the substrate surface. Average size of these pillars are found to be less than 15 nm. These pillars are very evenly distributed and forming a thin film onto the substrate surface. On the other hand, the PEG template TiO_2 film is more disordered possesses with several cracks which are clearly visible onto the surface. The particles of TiO_2 are also, at places, aggregated. Moreover, the BET pore size analysis shows that the pore size of these two catalysts is in the order of 4–8 nm and the Scherrer diameter indicates that the particle diameter is in the order of 21–29 nm. Therefore, it is assumed that a regular network is obtained onto the substrate surface and, possibly, the titania is forming a Nanopillars onto the substrate with a maximum size of ~30 nm.

The 3D AFM images of S1 and S2 samples are shown in Fig. 1. The figure indicates that S1 is composed with homogeneous distribution of nano-TiO_2 pillars on the substrate surface indicating that the films are optically smooth. However, a non-uniform distribution of particles was observed with catalyst S2. Further, the average height of the pillars was found to be 180 and 40 nm respectively for the S1 and S2 samples. These results are in good agreement with the above SEM observation. Moreover, the average roughness (Ra) and root mean square roughness (Rq) parameters were calculated and found to be 3.523, 14.06 nm and 2.708, 4.668 nm, respectively for S1 and S2 samples.

The XRF analytical data was obtained for the S1 and S2 photo-catalysts along with the blank borosilicate glass and presented elsewhere [40]. The results show that the S1 and S2 samples are possessed with 2.65 and 4.29 weight percentage of Ti. This clearly indicates that Ti is significantly immobilized onto the substrate surface. Further, the percent of Ti is increased significantly with the S2 sample suggesting that the filler media PEG greatly supported the network formation and propagation.

The XPS spectra of S1 and S2 is obtained and presented graphically in Fig. 4S and also reported elsewhere [40]. Figure reveals that the thin films are predominantly composed with Ti and O elements as analyzed onto the surface region. Characteristic binding energy peaks of Ti (2p) and O (1s) are occurred with these two catalysts Fig. 4S (inset). The peaks at 458.5 and 464.5 eV corresponds to the splitting electrons of Ti^{4+} ($2p_{3/2}$) and Ti^{4+} ($2p_{1/2}$), confirms the titanium is present in its fully oxidized state i.e., Ti^{4+} [46]. The binding energies of O (1s) (529.7 and 529.8 eV) are assigned to the surface-adsorbed oxygen, such as O_2^{2-} or O^- from the defect oxide or hydroxyl-like group [47]. This further indicates the titanium is present with its particulate form and, possibly, forming Nanopillars onto the borosilicate glass surface.

The BET specific surface area of S1 and S2 catalyst are found to be 5.217 and 1.420 m^2/g, respectively [40]. Similarly, the pore size was found to be 7.77 and 4.16 nm for the samples S1 and S2, respectively. It is observed that although the specific surface area of the catalyst is decreased with the thin films in presence of PEG however, the meso-pore size is decreased significantly. This enhances the possibility of the pollutants to trap within the pores and show a better catalytic activity. The PEG enables to provide a good filler media which subsequently provides a regular titanium network formation and propagation revealing much lower pore size of the catalyst as obtained for S2 catalyst.

3.2. Photocatalytic degradation of micro-pollutants

3.2.1. Effect of pH in the degradation of DFS and TC

The effect of pH is an important parameter in the degradation/oxidation of pollutants since it deals the mechanism involved on the surface of photocatalyst. The catalytic action is greatly influenced with the sorption of pollutants on to a catalyst surface and sorption is highly dependent to the solution pH. The catalyst surface charge, the size of the catalyst aggregates as well the positions of conductance and valence bands are influenced with pH [48]. Therefore, a pH dependence degradation of DFS and TC is conducted varying the pH from pH 4.0 to 10.0. The percent degradation of micro-pollutant is calculated and results are presented graphically in Fig. 2a and b respectively for the diclofenac sodium and tetracycline hydrochloride. Results are obtained at the completion of 2 h of irradiation. It is obvious that the presence of thin film (S1 and S2) samples greatly enhance the degradation of DFS and TC comparing to UV only irradiation. Quantitatively, a very high percent degradation of DFS was obtained at pH 6.0 and this was 7.75%, 52.03% and 63.10% for the UV only, S1 and S2 samples, respectively. However, increasing further the pH even up to 10, the degradation of DFS was decreased to its percent removal values of 6.90%, 31.03% and 41.38%, respectively for UV, S1 and S2 samples. It was further, noted that very low percent oxidation of DFS was not affected significantly with change in solution pH with the UV only treatment. The surface properties of S1 and S2 greatly influence the percent degradation of DFS. The pH_{PZC} of the powders T1 and T2 (obtained by the sols S1 and S2 solutions) is found to be 6.9 [40]. It is assumed that the TiO_2 surface remains positively charged in acidic media (pH < 6.9) and negatively charged in alkaline solutions (pH > 6.9) (*cf* Eq. (3)).

$$\equiv SOH_2^+ \rightarrow \equiv \underset{pH_{PZC}}{SOH^0} \rightarrow \equiv SO^- \tag{3}$$

On the other hand, diclofenac is having low dipole moment and acid dissociation constant value pK_a: 4.21 [49]. This implies that diclofenac carries negative charge beyond pH 4.2. Therefore, beyond pH 4.2 a sharp increase in the degradation of DFS is encountered due to strong electrostatic attraction of DFS by the surface since the catalyst surface carries net positive charge. However, further increase in pH i.e., beyond pH 6.0 i.e., up to pH 10.0, the surface of TiO_2 also carries a negative charge therefore; because of electrostatic repulsion the DFS molecule could not approach to the catalyst surface effectively which render in sharp

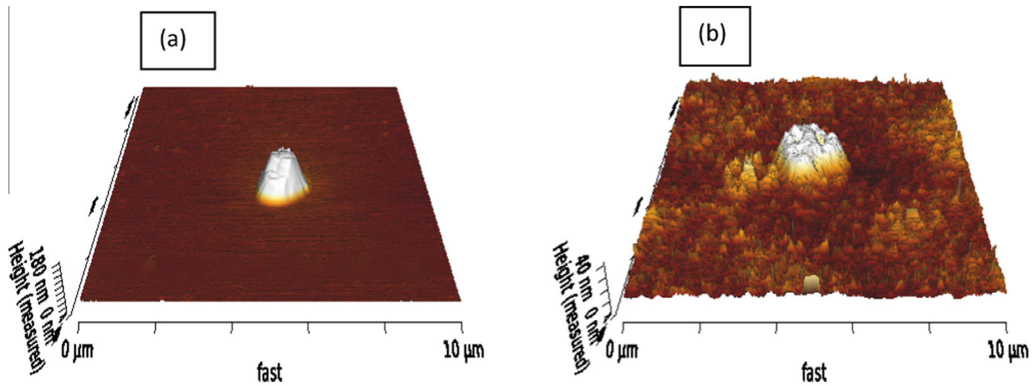

Fig. 1. 3D AFM images of S1 and S2 samples at the scale of 10 × 10 μm^2.

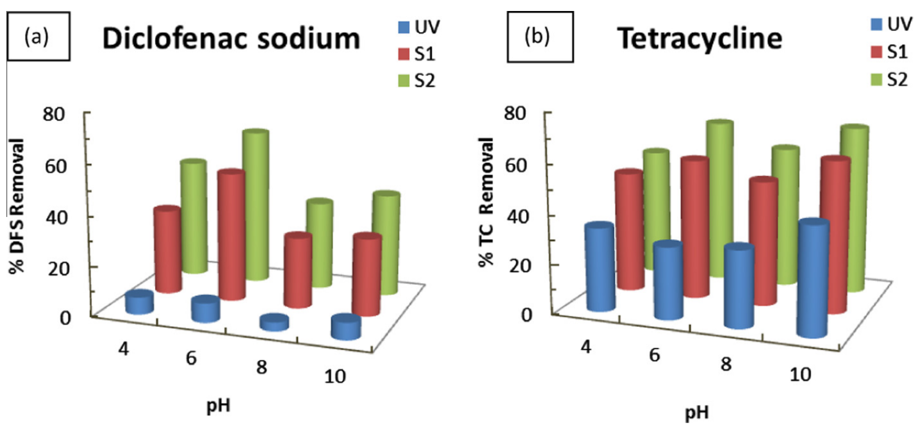

Fig. 2. Effect of pH in the photocatalytic degradation of (a) diclofenac sodium; and (b) tetracycline.

decrease in percent degradation of DFS. It is assumed that the diclofenac molecule easily enters within the interspace of cavities and reacts with hydroxyl radicals generated by the UV radiations at an increased rate. However, at higher pH conditions the DFS molecules predominantly lies in the bulk solution where the concentration of hydroxyl radicals is insignificant hence; decreases the percent removal of DFS [50]. Similar findings were reported for the degradation of DFS in the continuous photocatalytic membrane reactor employing UV-C radiations [23]. In contrast, previously it was found that diclofenac was mineralized with higher rate at pH 4.0 comparing to pH ∼7.0 using photocatalytic process [51].

Similarly, the oxidative percent removal of TC is relatively low at pH 4.0 however, it is increased significantly at higher pH values i.e., pH 6.0 and reached to a maximum percent removal at pH 10.0 as 43.37%, 61.06%, 68.14% efficiency is achieved by the UV, S1 and S2 samples, respectively (*cf* Fig. 2b). TC is having different functional groups with the pK_{a1}, pK_{a2} and pK_{a3} values of 3.3, 7.7 and 9.7, respectively [52]. Between pH 3.3 and 7.7, TC exists as a zwitterion (TCH_2^0 or $TCH_2^{0\,+\,-}$), due to loss of a proton from phenolic diketone moiety. At solution pH greater than 7.7, TC exists as anion (TCH^- or $TCH^{+\,-\,-}$). Further, at pH 9.7 it exists as di-anionic form (TC^{2-} or $TC^{0\,-\,-}$) by the loss of another proton from the tri-carbonyl system and phenolic diketone moiety [52]. Since both species TCH_2^0 and TCH^- of tetracycline contains with positively charged group in their structure and it is likely that these molecules are arranged at the surface so that the positively charged group is located very close to the surface, leading the negatively charged one(s) as far as possible from the surface, which reveals that electrostatic attraction may play an important role in the sorption of TCH_2^0 and TCH^- species dominantly within the pH region 6.0 to 10.0 [53]. Consequently, this causes to enhance the degradation of TC using the photocatalyst. Previously, it was found that the photo-electro-Fenton process was found to be effective within the pH range ∼3.0–7.0 comparing to the Electro-Fenton at low pH values [32]. However, the present study is useful in the treatment of TC at a wide range of pH from moderate to high pH region ∼6.0–10.

3.2.2. Effect of micro-pollutant concentration

Further, the effect of micro-pollutant concentration is studied at a wide range of pollutant concentrations i.e., 1.0–5.0 mg/L for DFS and 1.0–20.0 mg/L for TC at pH 6.0. The results are presented as percent removal of micro-pollutants as a function of initial concentrations and returned in Fig. 3a and b respectively for DFS and TC. In general it is observed that increasing the micro-pollutant concentration the percent degradation is decreased. More quantitatively, increasing the DFS concentration from 1.0 to 5.0 mg/L the percent DFS removal is decreased from 63.10% to 40.14% using S2 samples. Similarly, TC is decreased from 79.17% to 33.41% for the increase in TC concentration from 1.0 to 20.0 mg/L using S2 catalyst. The increase in concentration greatly suppresses the percent removal of micro-pollutants. This is due to the fact that effective contact possibilities with the MPs molecules is increased significantly at lower concentrations of MPs, however, the percent supply of active species are decreased at higher pollutant concentrations. It further indicates that the thin films S1 and S2 show significantly higher photocatalytic activity in the efficient degradation of DFS or TC from aqueous solutions comparing to the UV only irradiated samples. Further, S2 sample, which was made by the PEG template synthesis, showed an enhanced photocatalytic activity than the S1 sample. This is due to the fact that S2 sample possessed with small pores, which effectively traps the micro-pollutants and the photo induced radicals oxidizes efficiently the micro-pollutant molecules. The immobilization of nano-TiO_2 renders an enhanced applicability since the use of thin films provides additional advantage of easy phase separation. It was reported previously that increasing the micro-pollutant concentration saturates the TiO_2 surface hence reduces the photonic efficiency which causes deactivation of photocatalyst [54]. Similarly, the percent degradation of TC was greatly decreased on increasing the initial concentration of TC from 25 to 100 mg/L using the TiO_2-plasma reactor [34].

3.2.3. Kinetics of photocatalytic degradation of micro-pollutants

Kinetics of photo-catalytic degradation of DFS and TC is studied. The C_t/C_0 values are obtained and presented graphically in Fig. 4a and b, respectively for the diclofenac sodium and tetracycline (where C_0 is initial concentration of micro-pollutant and C_t is the concentration of micro-pollutant at time 't'). It is evident from the figures that a sharp decrease in degradation of MPs is observed in presence of thin films S1 and S2 whereas the UV irradiation showed almost no degradation of diclofenac. However, the tetracycline is degraded partly since the C_t/C_0 is having 0.71 at the completion of 2 h of irradiation by the UV only irradiation. The C_t/C_0 values were found to be 0.70 and 0.59 (for diclofenac sodium) and 0.43 and 0.34 (for tetracycline) for the S1 and S2 samples, respectively. Comparatively, significant lower values of C_t/C_0 both for the DFS and TC using S2 samples was obtained comparing to the S1 samples which again indicated the affinity of these micro-pollutants toward the thin film surfaces and enhanced photocatalytic degradation of MPs was occurred at the catalyst surface. Among these two pollutants studied, photocatalytic degradation of diclofenac sodium was less than the tetracycline. This is due to relative affinities of these two micro-pollutants toward the thin films as well as the stability of organic compounds in aqueous solutions.

The kinetics of degradation is represented using the known pseudo-first order rate equation (Eq. (4)):

$$r = -\frac{d[MP]}{dt} = k_{app}[k_{photolysis} + k_{photocatalysis}][MP] = k_{app}[MP] \tag{4}$$

where [MP] represents the concentration of micro-pollutant and k_{app} is the pseudo-first-order rate constant. This implies that the k_{app} is dependent to the concentration of micro-pollutant.

Integration of Eq. (4)with the extreme conditions i.e., at $t = 0$ the $[MP] = C_0$. Eq. (4) results to Eq. (5):

$$LN\left(\frac{C_0}{C_t}\right) = k_{app} \cdot t \tag{5}$$

Straight lines were drawn between the $LN(C_0/C_t)$ against time 't'. Results obtained are presented graphically in Fig. 4a and b (inset), respectively for the diclofenac sodium and tetracycline (Initial concentration of DFS or TC: 5.0 mg/L and pH: 6.0). The pseudo-first-order rate constants are evaluated at different concentrations for the UV, S1 and S2 samples and results are returned in Table 1. Table 1 clearly indicate that increasing the concentration of micro-pollutant the k_{app} values decreases. Therefore, the low initial concentration of micro-pollutants is found to be efficient, at least, in the photo-catalytic degradation of DFS or TC using the thin films. Similar to previous studies, the S2 sample possess higher removal efficiency comparing to the S1 samples. This again reaffirms the potential use of template synthesis of thin films using the PEG as filler media. On the other hand, photolysis only shows very low values of rate constant for tetracycline whereas since it shows almost negligible degradation of DFS hence, the rate constant values are not computed. It was reported previously that the degradation of DFS was decreased significantly with increasing the initial concentration of DFS and explained with the fact that there could be a competition for the absorption of limited number of available photons by the DFS molecules [11]. Once the initial concentration of DFS was increased, the number of available photons was not altered therefore, the number of photons available per molecule of DFS apparently decreased, so the degradation rate of DFS was decreased.

Photocatalytic oxidation kinetics of micro-pollutants is modeled with the Langmuir–Hinshelwood (L–H) equation. This includes the adsorption properties of adsorbate species on the photocatalyst surface. The derived Eq. (7) is used to its linear form:

$$r_0 = \frac{k_r \cdot K \cdot C_0}{1 + K \cdot C_0} \tag{6}$$

or $$\frac{1}{r_0} = \frac{1}{K \cdot k_r} \cdot \frac{1}{C_0} + \frac{1}{k_r} \tag{7}$$

where '$1/r_0$' is the dependent variable, '$1/C_0$' the independent variable, $1/k_r$ is the linear coefficient and $(1/(k_r K))$ the angular coefficient of the straight line. From this model, the L–H adsorption constant and the rate constant are computed plotting $1/r_0$ against $1/C_0$ [55]. The k_r (mg/L/min) and K (L/mg) values are found to be 0.014 and 0.508 (R^2: 0.532; for S1) and 0.0243 and 0.685 (R^2: 0.704; for S2 sample), respectively in the oxidation of diclofenac. Whereas, for the TC the corresponding values of k_r and K are found to be 0.064 and 6.031 (R^2: 0.991; for S1 sample) and 0.101 and 6.748 (R^2: 0.998; for S2 samples), respectively. The values obtained for the DFS is having very low R^2 values. However, the L–H kinetics

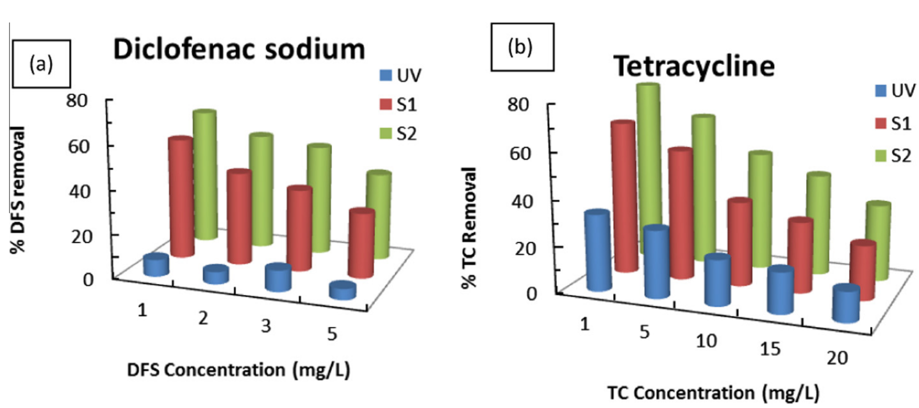

Fig. 3. Effect of concentration in the photocatalytic degradation of (a) diclofenac sodium; and (b) tetracycline.

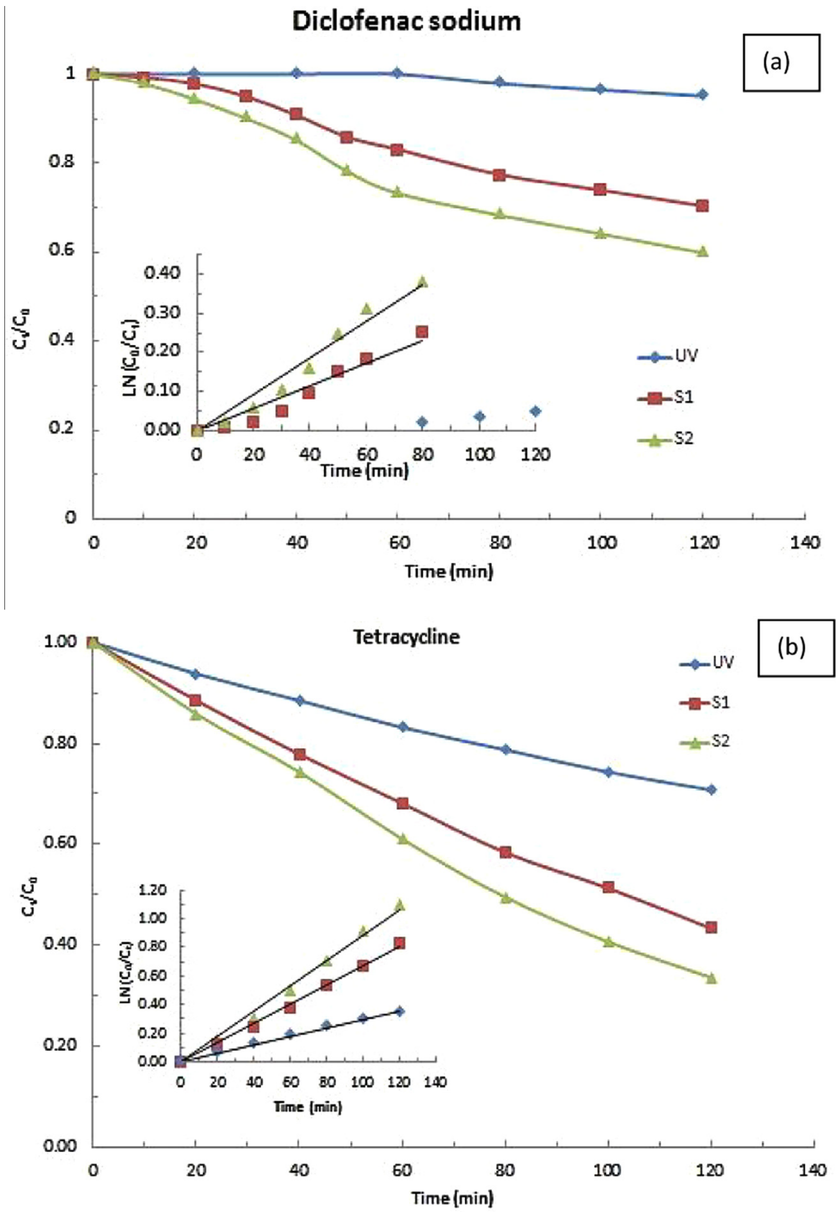

Fig. 4. Photocatalytic degradation of (a) diclofenac sodium; and (b) tetracycline as a function of time.

Table 1
Kinetic data obtained in the photo-catalytic degradation of micro-pollutants using thin films.

Samples	Pseudo-first-order rate constant ($k_{app} \times 10^{-3}$/min)								
	Diclofenac sodium (Initial concentrations)				Tetracycline (Initial concentrations)				
	1.0	2.0	3.0	5.0	1.0	5.0	10.0	15.0	20.0
UV only	–	–	–	–	3.5 (0.991)	3.0 (0.998)	1.9 (0.992)	1.5 (0.983)	1.1 (0.993)
S1	9.9* (0.984)	4.6 (0.914)	4.0 (0.941)	2.9 (0.930)	8.9 (0.998)	6.7 (0.997)	3.9 (0.999)	3.0 (0.999)	2.2 (0.998)
S2	15.1* (0.997)	7.5 (0.970)	6.7 (0.973)	4.7 (0.961)	12.7 (0.996)	8.8 (0.993)	6.1 (0.999)	4.8 (0.998)	3.4 (0.997)

R^2 values are given in parenthesis.
* Values obtained using initial 40 min of contact.

is fitted reasonably well to the photocatalytic degradation of tetracycline.

3.2.4. Mineralization of micro-pollutants

Further, the mineralization of DFS and TC was studied varying the micro-pollutant concentrations from 1.0 to 5.0 mg/L for DFS and 1.0 to 10.0 mg/L for TC at constant pH 6.0 employing the UV only, S1 and S2 photo-catalysts. Results are obtained at the end of 2 h of photo-irradiation. Percent of TOC removal as a function of micro-pollutant concentration is presented graphically in Fig. 5a and b for the diclofenac sodium and tetracycline, respectively. It is evident from the figure that increasing the concentration of micro-pollutants, a sharp decrease in TOC is observed. Quantitatively, increasing the concentration of diclofenac sodium from 1.0 to 5.0 mg/L the percent of TOC is decreased from 23.33% to 12.23% using the S2 thin film. Whereas increasing the tetracycline concentration from 1.0 to 20.0 mg/L the respective decrease in percent TOC is obtained from 40.53% to 12.56% using the S2 thin film. It is to be noted that a partial mineralization of these pollutants is achieved using the photo catalytic degradation employing S1 and S2 thin films. However, it is seen that the multiple use of thin films is quite possible hence; a repeated application could achieve a complete mineralization of diclofenac or tetracycline from aqueous solutions.

Similar to the concentration dependence study, the S1 thin film showed significantly lower efficiency in terms of percent TOC removal. The UV only experiments showed almost negligible TOC removal of diclofenac sodium however; a partial but low removal of tetracycline was obtained using the UV only treatment as compared to the S1 and S2 photo-catalysts.

3.2.5. Effect of scavengers

In order to pinpoint the photocatalytic action of employed catalyst the effect of scavengers in the degradation of DFS and TC was studied using variety of scavengers as to scavenge the radical species *viz.*, $^{\cdot}OH$ or $O_2^{\cdot-}$. It was reported that 2-propanol and HCO_3^- are good scavengers of the $^{\cdot}OH_{bulk}$ ($^{\cdot}OH$ in aqueous medium) or surface $^{\cdot}OH$ radicals [55–57]. Whereas the sodium azide (NaN_3) is known to scavenge the singlet oxygen produced readily by the interaction of superoxide radical and photogenerated holes (Eq. (8)):

$$O_2^{\cdot-} + h^+ \rightarrow {}^1O_2 \quad (8)$$

The singlet oxygen is also a highly reactive species and causes to degrade the pollutants in aqueous solutions [58]. Therefore, the study is extended in the photo-catalytic degradation of DFS or TC (5.0 mg/L) in presence of 2-propanol, sodium azide and sodium bicarbonate (1000 mg/L) using the S1 and S2 thin films. The pollutant samples are irradiated for 2 h and then subjected for the estimation of pollutant concentration using UV–Vis and HPLC for tetracycline and DFS, respectively. The percent degradation of DFS and TC is obtained and presented graphically (*cf* Fig. 6) with respect to the presence of these scavengers. Results clearly demonstrated that the presence of sodium azide could not affect in the degradation of DFS and TC using the S1 or S2 thin films. This implies that the degradation of these pollutants is not proceeding through oxidation by the singlet oxygen species. However, the other studies, indicated that bisphenol A (BPA) was scavenged significantly in presence of NaN_3 and suggested that singlet oxygen degraded the BPA directly [57,59]. On the other hand, the scavengers, 2-propanol and bicarbonate significantly suppressed the catalytic activity of these thin films since a marked decrease in percent removal of DFS and TC was recorded. This implies that the $^{\cdot}OH$ radicals predominantly attributing the degradation of DFS or TC from aqueous solutions. Similar, results were shown previously in the photocatalytic oxidation of TC using TiO_2 [35,36].

3.2.6. Effect of interfering ions

Similarly, the natural waste water matrix was simulated to assess the applicability of thin film (S2) in the photocatalytic degradation of DFS and TC from aqueous solutions. Therefore, the photocatalytic degradation of DFS or TC using the S2 thin film was conducted in presence of several interfering ions (5.0 mg/L) including the cadmium nitrate, copper sulfate, zinc chloride, sodium chloride, sodium nitrate, sodium nitrite, glycine, oxalic acid and EDTA. The samples are irradiated for 2 h at pH 6.0 and the initial concentration of DFS or TC was kept constant to 1.0 mg/L. The diclofenac sodium was analyzed with the HPLC whereas tetracycline concentration was obtained with the UV–Vis spectrophotometer. The percent removal of micro-pollutant is presented as a function of interfering ions and returned in Fig. 7a and b respectively for the diclofenac sodium and tetracycline. It is observed that the presence of these ions hamper to some extent the degradation of DFS or TC but not at greater extent. However, the presence of nitrate and nitrite as in the form of sodium or even sodium chloride salts scavenges the photocatalytic degradation of both the pollutants. It was previously reported that the presence of nitrate ions with water readily produces the $^{\cdot}OH$ radicals with the UV irradiation [60]. Therefore, the $^{\cdot}OH$ radicals are supposed to enhance the DFS or TC degradation. However, the contribution rate of self-sensitization photo-oxidation via $^{\cdot}OH$ was reported to be 14.99%. The photo-degradation of DFS was predominantly attributed to direct photolysis. Hence, the effect via $^{\cdot}OH$ radicals plays an insignificant role in overall photo-degradation process. Further, in presence of nitrate ions there could be an enhanced competition for the UV radiations for limited number of available photons [28]. Similar to nitrate the nitrite also inhibit the degradation of

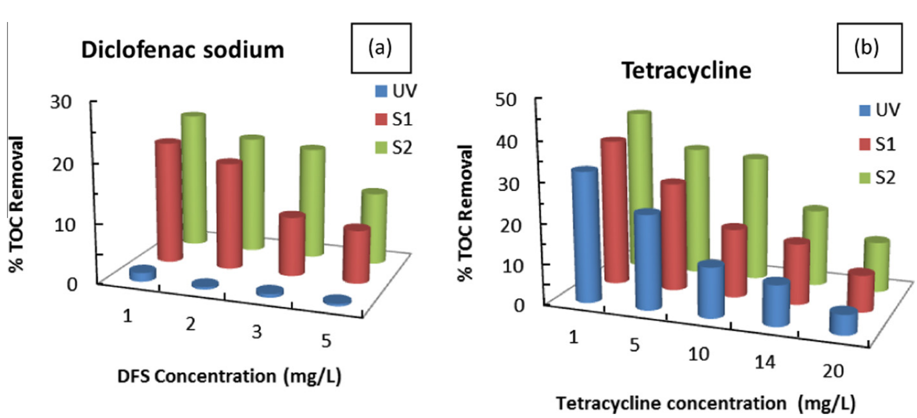

Fig. 5. Percent TOC removal of (a) diclofenac sodium; and (b) tetracycline as a function of micro-pollutant concentration in the photo-catalytic degradation using thin films.

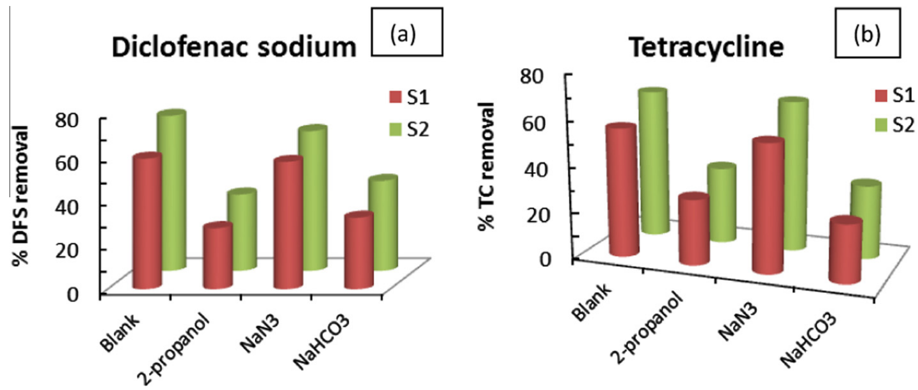

Fig. 6. Effect of scavengers in the photocatalytic degradation of (a) diclofenac sodium; and (b) tetracycline using the thin films.

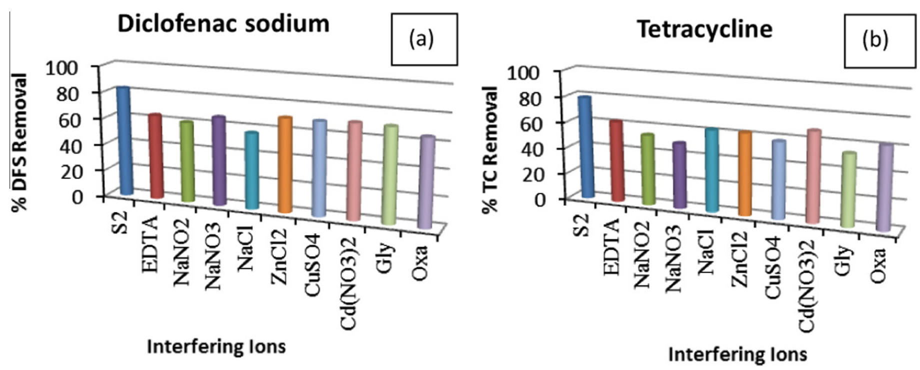

Fig. 7. Photocatalytic degradation of (a) diclofenac sodium; and (b) tetracycline in presence of interfering ions using S2 thin film.

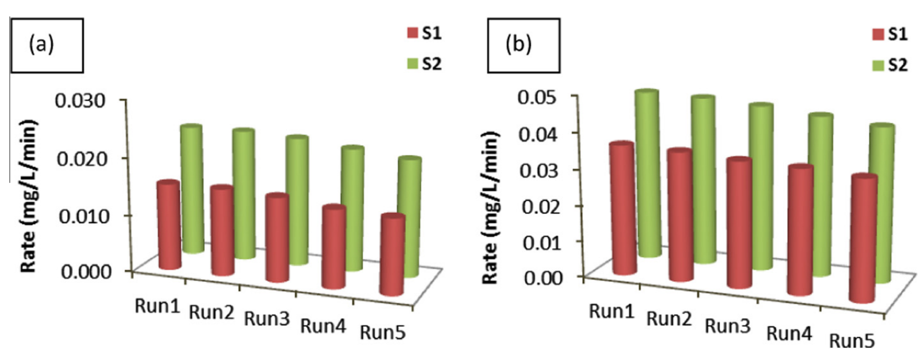

Fig. 8. Degradation rate of (a) diclofenac sodium; and (b) tetracycline using S1 and S2 with respect to repetitive use.

diclofenac and TC [28]. Previously, it was reported that EDTA is a good scavenger for h^+ from the VB and caused a significant decrease in the degradation of pollutants from aqueous solutions [61]. However, in this study EDTA is not suppressed significantly the degradation of either DFS or TC hence, the predominant pathway of degradation is by the ·OH radicals. Moreover, the competitive adsorption of cations or anions towards the surface of Nanopillars TiO_2 greatly affects the catalytic action of photo-catalyst [35].

3.2.7. Reusability test of the thin films

The reusability test for the two thin films S1 and S2 was conducted for their degradation of diclofenac sodium and tetracycline with a fixed initial concentration (5.0 mg/L) at pH 6.0 for 2 h irradiation for five consecutive experimental runs. The rate of degradation of these pollutants for each repetitive cycle are computed and presented graphically in Fig. 8a and b respectively for the diclofenac sodium and tetracycline. The results showed a negligible drop in the rate of degradation of these micro-pollutants within five experimental runs using S1 sample as: from 0.0029 to 0.0026 mg/L/min and 0.036 to 0.032 mg/L/min for DFS and TC, respectively. Similarly, with S2 thin films, the rate of degradation was decreased from 0.0040 to 0.0037 mg/L/min and 0.048 to 0.043 mg/L/min respectively, for DFS and TC. Thus the reduction in catalytic activity of these thin films was found to be 9.52%, 7.81% (using S1) and 7.02%, 8.0% (using S2) for the degradation of DFS and TC, respectively at the end of five cycles of photocatalytic treatment. These results clearly show that the thin film samples S1 and S2 could be reused without much decline in activity which conveys the cost effective process and makes it useful for practical implications in the photocatalytic degradation of diclofenac sodium and tetracycline from aqueous solutions.

4. Conclusions

The Nanopillars of TiO_2 are obtained onto borosilicate glass substrates. The sol–gel template synthesis was conducted using PEG as modifier. The two thin films i.e., S1 and S2 were obtained with and without PEG. XRD data revealed that anatase phase of Nanopillar TiO_2. The IR analysis indicated the presence of –OH group with both the catalyst samples. The XRF data enabled the presence of titanium element in the S1 and S2 samples. Moreover, the XPS analysis indicated the presence of Ti and O elements. Similarly, BET surface area were found to be 5.217 and 1.420 m^2/g, with the pore size 7.77 and 4.16 nm, respectively for the S1 and S2 thin films. SEM images showed fine grains of TiO_2 were very evenly distributed onto the substrate and forming a thin layer of TiO_2 particles for S1 sample. Whereas S2 sample possessed relatively disordered surface structure indicating the film has several micro-cracks onto the surface. AFM analytical data showed that the mean pillar size of TiO_2 particulate was *Ca* 180 and 40 nm respectively for the S1 and S2 samples. Moreover, the average roughness (Ra) and root mean square roughness (Rq) were found to be 3.523, 14.06 nm and 2.708, 4.668 nm, respectively for S1 and S2 samples. The photo-catalytic activity of these photo-catalyst showed relatively high degradation of DFS was occurred at pH 6.0 whereas the TC was degraded effectively within the pH region 6.0–10.0. The effect of pollutant concentration study revealed that decreasing the pollutant concentration favored greatly the percent removal of DFS and TC. Similarly, the mineralization of these micro-pollutants was increased with decreasing the pollutant concentration. The degradation process followed pseudo-first order rate kinetics and data was applicable with the Langmuir–Hinshelwood rate kinetics. The L–H kinetics was fitted reasonably well to the photocatalytic degradation of tetracycline whereas the DFS showed distorted kinetic results. Further, the presence of several cations and anions were affected to some extent the degradation efficiency of DFS or TS by the photo-catalytic degradation using the S2 catalyst. Moreover, the hydroxyl radical scavengers, 2-propanol and sodium bicarbonate greatly affected the catalytic activity of these thin films whereas the singlet oxygen scavenger sodium azide could not affect the catalytic activity of S1 and S2 at least in the photocatalytic degradation of DFS and TC from aqueous solutions. Overall the S1 and S2 samples showed very high percent degradation of DFS and TC comparing to the UV photolysis. Moreover, the S2 showed relatively enhanced percent removal of DFS and TC as compared to the S1 thin film. The reusability test showed only negligible drop in catalytic activity of the thin films even at the end of five repeated cycles of degradation of DFS and TC from aqueous solutions inferred the greater applicability of thin films. The thin films may further enhance the applicability of photo-catalyst in separation of slurry or to overcome the shadowing effect often occur with powder samples.

Acknowledgements

This work was supported by the National Research Foundation of Korea (NRF) grant funded by the Korea government (MEST) (No. 2012R1A2A4A01001539). One of the authors C. L also wishes to acknowledge UGC-NERO for the financial support as in the form of Research Project (vide No.: F.5-93/2014-15/MRP/NERO).

Appendix A. Supplementary data

Supplementary data associated with this article can be found, in the online version, at http://dx.doi.org/10.1016/j.cej.2015.07.032.

References

[1] S.A. Snyder, P. Westerhoff, Y. Yoon, D.L. Sedlak, Pharmaceuticals, personal care products, and endocrine disruptors in water: implications for the water industry, Environ. Eng. Sci. 20 (2003) 449–469.
[2] J. Niu, S. Ding, L. Zhang, J. Zhao, C. Feng, Visible-light-mediated $Sr–Bi_2O_3$ photocatalysis of tetracycline: kinetics, mechanisms and toxicity assessment, Chemosphere 93 (2013) 1–8.
[3] K.A. Landry, T.H. Boyer, Diclofenac removal in urine using strong-base anion exchange polymer resins, Water Res. 47 (2013) 6432–6444.
[4] J. Lienert, T. Buerki, B.I. Escher, Reducing micropollutants with source control: substance flow analysis of 212 pharmaceuticals in faeces and urine, Water Sci. Technol. 56 (2007) 87–96.
[5] S. Larcher, V. Yargeau, Biodegradation of 17α-ethinylestradiol by heterotrophic bacteria, Environ. Pollut. 173 (2013) 17–22.
[6] P.C. Heaton, S.R. Fenwick, D.E. Brewer, Association between tetracycline or doxycycline and hepatotoxicity: a population-based case – Control study, J. Clin. Pharm. Ther. 32 (2007) 483–487.
[7] P. Gao, M. Munir, I. Xagoraraki, Correlation of tetracycline and sulfonamide antibiotics with corresponding resistance genes and resistant bacteria in a conventional municipal wastewater treatment plant, Sci. Total Environ. 173 (2012) 421–422.
[8] W. Yang, Z. Tang, F. Zhou, W. Zhang, L. Song, Toxicity studies of tetracycline on *Microcystis aeruginosa* and *Selenastrum capricornutum*, Toxicol. Pharmacol. 35 (2013) 320–322.
[9] H.Y. Kim, J. Jeon, J. Hollender, S. Yu, S.D. Kim, Aqueous and dietary bioaccumulation of antibiotic tetracycline in D. magna and its multigenerational transfer, J. Hazard. Mater. 279 (2014) 428–435.
[10] D. Vogna, R. Marotta, A. Napolitano, R. Andreozzi, M. d'Ischia, Advanced oxidation of the pharmaceutical drug diclofenac with UV/H_2O_2 and ozone, Water Res. 38 (2004) 414–422.
[11] Y. Zhang, S.Y. Geissen, C. Gal, Carbamazepine and diclofenac: removal in wastewater treatment plants and occurrence in water bodies, Chemosphere 73 (2008) 1151–1161.
[12] J.M. Herrmann, Heterogeneous photocatalysis: fundamentals and applications to the removal of various types of aqueous pollutants, Catal. Today 53 (1999) 115–129.
[13] C. Martínez, L.M. Canle, M.I. Fernández, J.A. Santaballa, J. Faria, Aqueous degradation of diclofenac by heterogeneous photocatalysis using nanostructured materials, Appl. Catal. B: Environ. 107 (2011) 110–118.
[14] R. Bort, X. Ponsoda, R. Jover, M.J. Gomez-Lechon, R.J.V. Castell, Diclofenac toxicity to hepatocytes: a role for drug metabolism in cell toxicity, J. Pharmacol. Exp. Ther. 288 (1998) 65–72.
[15] J.L.G. Oaks, M. Virani, M.Z. Watson, R.T. Meteyer, C.U. Rideout, B.A. Shivaprasad, H.L. Ahmed, S. Chaudhry, M.J.I. Arshad, M. Mahmood, S. Ali, A.A.A. Khan, Diclofenac residues as the cause of vulture population decline in Pakistan, Nature 427 (2004) 630–633.
[16] A.C. Mehinto, E.M. Hill, C.R. Tyler, Uptake and biological effects of environmentally relevant concentrations of the nonsteroidal anti-inflammatory pharmaceutical diclofenac in rainbow trout (*oncorhynchus mykiss*), Environ. Sci. Technol. 44 (2010) 2176–2182.
[17] I. Vergili, Application of nanofiltration for the removal of carbamazepine, diclofenac and ibuprofen from drinking water sources, J. Environ. Manage. 127 (2013) 177–187.
[18] K. Ikehata, N.J. Naghashkar, M.G. El-Din, Degradation of aqueous pharmaceuticals by ozonation and advanced oxidation processes: a review, Ozone Sci. Eng. 28 (2006) 353–414.
[19] S.D. Kim, J. Cho, I.S. Kim, B.J. Vanderford, S.A. Snyder, Occurrence and removal of pharmaceuticals and endocrine disruptors in South Korean surface, drinking and waste waters, Water Res. 41 (2007) 1013–1021.
[20] E.S. Rigobello, A. DiBernardo Dantas, E.M. DiBernardo Luiz Vieira, Removal of diclofenac by conventional drinking water treatment processes and granular activated carbon filtration, Chemosphere 92 (2013) 184–191.
[21] J. Radjenovic, M. Petrovic, F. Ventura, D. Barcelo, Rejection of pharmaceuticals in nanofiltration and reverse osmosis membrane drinking water treatment, Water Res. 42 (2008) 3601–3619.
[22] M.R. Boleda, M.T. Galceran, F. Ventura, Behavior of pharmaceuticals and drugs of abuse in a drinking water treatment plant (DWTP) using combined conventional and ultrafiltration and reverse osmosis (UF/RO) treatments, Environ. Pollut. 159 (2011) 1584–1591.
[23] V.C. Sarasidis, K.V. Plakas, S.I. Patsios, A.J. Karabelas, Investigation of diclofenac degradation in a continuous photo-catalytic membrane reactor. Influence of operating parameters, Chem. Eng. J. 239 (2014) 299–311.
[24] J. Rivas, O. Gimeno, T. Borralho, F. Beltrán, Influence of oxygen and free radicals promoters on the UV-254 nm photolysis of diclofenac, Chem. Eng. J. 163 (2010) 35–40.
[25] W. Wang, Y. Yu, T. An, G. Li, H.Y. Yip, J.C. Yu, P.K. Wong, Visible-light-driven photocatalytic inactivation of E. coli K-12 by bismuth vanadate nanotubes: bactericidal performance and mechanism, Environ. Sci. Technol. 46 (2012) 4599–4606.
[26] A. Aguinaco, F.J. Beltrán, J.F. García-Araya, A. Oropes, Photocatalytic ozonation to remove the pharmaceutical diclofenac from water: influence of variables, Chem. Eng. J. 189–190 (2012) 275–282.
[27] H. Yu, E. Nie, J. Xu, S. Yan, W.J. Cooper, W. Song, Degradation of diclofenac by advanced oxidation and reduction processes: kinetic studies, degradation pathways and toxicity assessments, Water Res. 47 (2013) 1909–1918.

[28] D. Zhang, R. Qiu, L. Song, B. Eric, Y. Mo, X. Huang, Role of oxygen active species in the photocatalytic degradation of phenol using polymer sensitized TiO_2 under visible light irradiation, J. Hazard. Mater. 163 (2009) 843–847.
[29] E. Marco-Urrea, M. Pérez-Trujillo, C. Cruz-Morató, G. Caminal, T. Vicent, Degradation of the drug sodium diclofenac by Trametes versicolor pellets and identification of some intermediates by NMR, J. Hazard. Mater. 176 (2010) 836–842.
[30] C.I. Brinzila, M.J. Pacheco, L. Ciríaco, R.C. Ciobanu, A. Lopes, Electrodegradation of tetracycline on BDD anode, Chem. Eng. J. 209 (2012) 54–61.
[31] N. Oturan, J. Wu, H. Zhang, V.K. Sharma, M.A. Oturan, Electrocatalytic destruction of the antibiotic tetracycline in aqueous medium by electrochemical advanced oxidation processes: effect of electrode materials, Appl. Catal. B: Environ. 140–141 (2013) 92–96.
[32] S. Liu, X.-R. Zhao, H.-Y. Sun, R.-P. Li, Y.-F. Fang, Y.-P. Huang, The degradation of tetracycline in a photo-electro-Fenton system, Chem. Eng. J. 231 (2013) 441–448.
[33] Y. Wang, H. Liu, G. Liu, Y. Xie, Oxidation of diclofenac by aqueous chlorine dioxide: identification of major disinfection byproducts and toxicity evaluation, Sci. Total Environ. 473–474 (2014) 437–445.
[34] D. He, Y. Sun, L. Xin, J. Feng, Aqueous tetracycline degradation by non-thermal plasma combined with nano-TiO_2, Chem. Eng. J. 258 (2014) 18–25.
[35] X.-D. Zhu, Y.-J. Wang, R.-J. Sun, D.-M. Zhou, Photocatalytic degradation of tetracycline in aqueous solution by nanosized TiO_2, Chemosphere 92 (2013) 925–932.
[36] C.V. Gomez-Pacheco, M. Sanchez-Polo, J. Rivera-Utrilla, J.J. Lopez-Penalver, Tetracycline degradation in aqueous phase by ultraviolet radiation, Chem. Eng. J. 187 (2012) 89–95.
[37] D. Xu, K. Liu, W. Shin, M. Chenn, B. Luo, L. Xiao, W. Gu, Ag-decorated $K_2Ta_2O_6$ nanocomposite photocatalysts with enhanced visible-light-driven degradation activities of tetracycline (TC), Ceram. Int. 41 (2015) 4444–4451.
[38] Y. Hong, A. Ren, Y. Jiang, J. He, L. Xiao, W. Shi, Sol–gel synthesis of visible-light-driven $Ni(1-x)Cu(x)Fe_2O_4$ photocatalysts for degradation of tetracycline, Ceram. Int. 41 (2015) 1477–1486.
[39] S.M. Lee, D. Tiwari, K.M. Choi, J.K. Yang, Y.Y. Chang, H.D. Lee, Removal of Mn(II) from aqueous solutions using manganese-coated sand samples, J. Chem. Eng. Data 54 (2009) 1823–1828.
[40] D. Tiwari, C. Lalhriatpuia Lalhmunsiama, S.-M. Lee, S.-H. Kong, Efficient application of nano-TiO_2 thin films in the photocatalytic removal of Alizarin Yellow from aqueous solutions, Appl. Surf. Sci. 353 (2015) 275–283.
[41] J.B. Hartmann, P. Mau, U. Witter, M. Tuempling, W. Hofmann, J.E. Nietzschmann, Degradation of the drug diclofenac in water by sonolysis in presence of catalysts, Chemosphere 70 (2008) 453–461.
[42] S. Rahim, M.S. Ghamsari, S. Radiman, Surface modification of titanium oxide nanocrystals with PEG, Sci. Iran. F 19 (2012) 948–953.
[43] A.J. Maira, J.M. Coronado, V. Augugliaro, K.L. Yeung, J.C. Conesa, J. Soria, Fourier transform infrared study of the performance of nanostructured TiO_2 particles for the photocatalytic oxidation of gaseous toluene, J. Catal. 202 (2001) 413–420.
[44] L.G. Devi, K.M. Reddy, Photocatalytic performance of silver TiO_2: role of electronic energy levels, Appl. Surf. Sci. 257 (2011) 6821–6828.
[45] S. Sugapriya, R. Sriram, S. Lakshmi, Effect of annealing on TiO_2 nanoparticles, Optik 124 (2013) 4971–4975.
[46] F.B. Li, X.Z. Li, The enhancement of photodegradation efficiency using Pt–TiO_2 catalyst, Chemosphere 48 (2002) 1103–1111.
[47] X.F. Lei, X.X. Xu, H. Yang, Preparation and characterization of Ag-doped TiO_2 nanomaterials and their photocatalytic reduction of Cr(VI) under visible light, Appl. Surf. Sci. 321 (2014) 396–403.
[48] M.N. Chong, B. Jin, C.W.K. Chow, C. Saint, Recent developments in photocatalytic water treatment technology: a review, Water Res. 44 (2010) 2997–3027.
[49] M. Meloun, S. Bordovska, L. Galla, The thermodynamic dissociation constants of four non-steroidal anti-inflammatory drugs by the least-squares nonlinear regression of multiwavelength spectrophotometric pH-titration data, J. Pharm. Biomed. Anal. 45 (2007) 552–564.
[50] A.G. Chakinala, P.R. Gogate, A.E. Burgess, D.H. Bremner, Intensification of hydroxyl radical production in sonochemical reactors, Ultrason. Sonochem. 14 (2007) 509–514.
[51] M.V. Bagal, P.R. Gogate, Degradation of diclofenac sodium using combined processes based on hydrodynamic cavitation and heterogeneous photocatalysis, Ultrason. Sonochem. 21 (2014) 1035–1043.
[52] P. Kulshrestha, R.F. Giese Jr., D.S. Aga, Investigating the molecular interactions of oxytetracycline in clay and organic matter: insights on factors affecting its mobility in soil, Environ. Sci. Technol. 38 (2004) 4097–4105.
[53] M.E. Parolo, M.C. Savini, J.M. Vallés, M.T. Baschini, M.J. Avena, Tetracycline adsorption on montmorillonite: pH and ionic strength effects, Appl. Clay Sci. 40 (2008) 179–186.
[54] M. Saquib, M. Muneer, TiO_2-mediated photocatalytic degradation of a triphenylmethane dye (gentian violet), in aqueous suspensions, Dyes Pigm. 56 (2003) 37–49.
[55] R.W. Matthews, Photooxidation of organic impurities in water using thin films of titanium dioxide, J. Phys. Chem. 91 (1987) 3328–3333.
[56] C. Chang, L. Zhu, Y. Fu, X. Chu, Highly active Bi/BiOI composite synthesized by one-step reaction and its capacity to degrade bisphenol A under simulated solar light irradiation, Chem. Eng. J. 233 (2013) 305–314.
[57] H. Wang, H. Yao, P. Sun, J. Pei, D. Li, C.-H. Huang, Oxidation of tetracycline antibiotics induced by Fe(III) ions without light irradiation, Chemosphere 119 (2015) 1255–1261.
[58] Y.Y. Li, J.S. Wang, B. Liu, L.Y. Dang, H.C. Yao, Z.J. Li, BiOI-sensitized TiO_2 in phenol degradation: a novel efficient semiconductor sensitizer, Chem. Phys. Lett. 508 (2011) 102–106.
[59] N. Zhang, G. Liu, H. Liu, Y. Wang, Z. He, G. Wang, Diclofenac photodegradation under simulated sunlight: effect of different forms of nitrogen and kinetics, J. Hazard. Mater. 192 (2011) 411–418.
[60] W.Z. Li, S.G. Lu, Z.F. Qiu, K.F. Lin, Clofibric acid degradation in UV_{254}/H_2O_2 process: effect of temperature, J. Hazard. Mater. 176 (2010) 1051–1057.
[61] X. Chang, J. Huang, C. Cheng, W. Sha, X. Li, G. Ji, S. Deng, G. Yu, Photocatalytic decomposition of 4-t-octylphenol over $NaBiO_3$ driven by visible light: catalytic kinetics and corrosion products characterization, J. Hazard. Mater. 173 (2010) 765–772.